Transient climate response estimated from radiative forcing and observed temperature change

J. M. Gregory[1,2] and P. M. Forster[3]

Received 13 May 2008; revised 19 September 2008; accepted 7 October 2008; published 10 December 2008.

[1] Observations and simulations (using the HadCM3 AOGCM) of time-dependent twentieth-century climate change indicate a linear relationship $F = \rho\Delta T$ between radiative forcing F and global mean surface air temperature change ΔT. The same is a good description of ΔT from CMIP3 AOGCMs integrated with CO_2 increasing at 1% per year compounded. The constant "climate resistance" ρ is related to the transient climate response (TCR, ΔT at the time of doubled CO_2 under the 1% CO_2 scenario). Disregarding any trend caused by natural forcing (volcanic and solar), which is small compared with the trend in anthropogenic forcing, we estimate that the real-world TCR is 1.3–2.3 K (5–95% uncertainty range) from the data of 1970–2006, allowing for the effect of unforced variability on longer timescales. The climate response to episodic volcanic forcing cannot be described by the same relationship and merits further investigation; this constitutes a systematic uncertainty of the method. The method is quite insensitive to the anthropogenic aerosol forcing, which probably did not vary much during 1970–2006 and therefore did not affect the trend in ΔT. Our range is very similar to the range of recent AOGCM results for the TCR. Consequently projections for warming during the twenty-first century under the SRES A1B emissions scenario made using the simple empirical relationship $F = \rho\Delta T$ agree with the range of AOGCM results for that scenario. Our TCR range is also similar to those from observationally constrained model-based methods.

Citation: Gregory, J. M., and P. M. Forster (2008), Transient climate response estimated from radiative forcing and observed temperature change, *J. Geophys. Res.*, *113*, D23105, doi:10.1029/2008JD010405.

1. Introduction

[2] Climate models show that continued emissions of greenhouse gases at or above current rates would cause climate change during the twenty-first century that would very likely be larger than that observed in the twentieth century, but there are great uncertainties about the size of the projected changes [*Meehl et al.*, 2007]. The magnitude of global climate change on multiannual timescales is conventionally measured by the global mean surface air temperature change ΔT. This quantity is useful because general circulation models (GCMs) suggest that many aspects of projected climate change scale with ΔT i.e., the change $\Delta V(\mathbf{x}, t)$ in some quantity V such as temperature or precipitation, as a function of geographical location $\mathbf{x}$ and time t, can be approximated as the product $\Delta V = P(\mathbf{x})\,\Delta T(t)$ of a constant spatial pattern P with a magnitude represented by ΔT [*Mitchell et al.*, 1999; *Huntingford and Cox*, 2000].

[3] The magnitude of the influence of a forcing agent is measured by its radiative forcing F, which is usually defined as the change in global mean net downward radiation at the tropopause caused by adding the forcing agent, either instantaneously, or with allowance for stratospheric adjustment. Recent work [*Shine et al.*, 2003; *Gregory et al.*, 2004; *Hansen et al.*, 2005; *Gregory and Webb*, 2008; *Williams et al.*, 2008; *Andrews and Forster*, 2008] suggests a more general definition of F as the net global mean heat flux into the climate system caused by the forcing agent without any climate response having occurred. In response to F, the magnitude of climate change is determined by a heat balance

$$N = F - \alpha\,\Delta T, \tag{1}$$

where N is the net heat flux into the climate system (W m^{-2}) and α is the climate sensitivity parameter (W m^{-2} K^{-1}) [e.g., *Gregory et al.*, 2004]. The term $\alpha\Delta T$ is the radiative response of the climate system to forcing on multiannual timescales. For a stable system $\alpha > 0$, so that if a positive forcing is imposed, such as by an increase in greenhouse gas concentrations, the net response is to lose more heat to space, and thus to tend to regain a steady state.

[4] When the system has reached a new steady state, in which $N = 0$ by definition, the magnitude of climate change depends on forcing and feedback according to $\Delta T = F/\alpha$. In the particular case of a doubling of the CO_2 concentration, for which $F = F_{2\times}$, ΔT is usually called the "equilibrium

[1]Department of Meteorology, Walker Institute for Climate System Research, University of Reading, Reading, UK.
[2]Met Office Hadley Centre, Exeter, UK.
[3]School of Earth and Environment, University of Leeds, Leeds, UK.

0148-0227/08/2008JD010405

climate sensitivity" $\Delta T_{2\times}$, with $\Delta T_{2\times} = F_{2\times}/\alpha$. The real climate is however never in a steady state, and during time-dependent change the rate of storage of heat also has an influence according to $\Delta T = (F - N)/\alpha$. On multiannual timescales, the storage of heat is overwhelmingly in the ocean [*Levitus et al.*, 2001; *Bindoff et al.*, 2007]. The heat balance indicates that during time-dependent climate change a greater rate of ocean heat uptake means a smaller ΔT for a given forcing.

[5] The important influence of heat storage on time-dependent change limits the practical usefulness of the equilibrium climate sensitivity in comparing simulations of climate change for the coming century. Therefore *Cubasch et al.* [2001] introduced a new metric, the "transient climate response" (TCR), defined as ΔT for the time of doubled CO_2 in a scenario in which CO_2 increases at 1% per year compounded. This is a commonly used idealized scenario for studies of climate change with atmosphere-ocean general circulation models (AOGCMs). At 1% per year, the time for doubling is 70 years, and in practice a time-mean over years 61–80 is used to evaluate the TCR ($=(F_{2\times} - N)/\alpha$). The TCR is less than $\Delta T_{2\times}$ ($=F_{2\times}/\alpha$) because the ocean heat uptake $N > 0$.

[6] One way to describe the ocean's role is as thermal inertia, with $N = C\mathrm{d}\Delta T/\mathrm{d}t$, where C is a constant heat capacity [*Frame et al.*, 2005]. For forced climate change on multidecadal timescales, the effective heat capacity C is greater than that of the ocean "mixed layer," and is actually not constant [*Keen and Murphy*, 1997; *Watterson*, 2000], because the ocean is not well-mixed, and the vertical profile of temperature change is time-dependent. An alternative description is $N = \kappa\Delta T$, where κ is the "ocean heat uptake efficiency" [*Gregory and Mitchell*, 1997; *Raper et al.*, 2002]. This formulation views the deep ocean as a heatsink, into which the surface climate loses heat in a way analogous to its heat loss to space. It permits the influences of climate feedback and ocean heat uptake to be compared, since α and κ have the same units. Like climate sensitivity, this formulation of ocean heat uptake is a model-based result. It is evident that its validity is restricted; it cannot be correct for steady state climate change, because $N \to 0$ as ΔT approaches its equilibrium value, so the efficiency of ocean heat uptake must decline. The formulation was proposed only as a description for a system in a time-dependent state forced by a scenario with a fairly steadily increasing forcing.

[7] When $N = \kappa\Delta T$ holds, we can write the heat balance of the climate system as $F = \rho\Delta T$ with $\rho \equiv \kappa + \alpha$, which we call the "climate resistance," because it is the reciprocal of the climate response. Unlike the formulation with a thermal inertia, the relationship $F = \rho\Delta T$ has no timescale. It suggests that climate change tracks radiative forcing. The aim of this paper is to examine the applicability of this relationship to projected and recent past climate change.

2. Results From 1% CO_2 Experiments

2.1. Climate Resistance and TCR

[8] Many AOGCMs in the Coupled Model Intercomparison Project phase 3 (CMIP3) of the World Climate Research Programme (WCRP) have been run under the 1% CO_2 scenario. Give forcing due to CO_2 alone, we can evaluate climate resistance ρ from the runs in this data set. To obtain ρ, we use ordinary least squares linear regression (OLS) of F against ΔT for years 1–70, during which CO_2 is increasing. In a set of 16 CMIP3 AOGCMs, the correlation coefficients for decadal-mean F with decadal-mean ΔT exceed 0.98 in almost every case, indicating that linearity is a very good assumption. Because of the high correlation, the results from OLS regression are practically identical regardless of whether ΔT or F is taken as the independent variable.

[9] We adopt a standard value of $F_{2\times} = 3.7$ W m^{-2} for the forcing due to doubled CO_2 [*Myhre et al.*, 1998], which is close to the average of AOGCM values reported by *Forster and Taylor* [2006]. AOGCMs actually have a spread of O(10)% in the 2 × CO_2 forcing [*Collins et al.*, 2006; *Forster and Taylor*, 2006]. Furthermore, *Gregory and Webb* [2008], *Williams et al.* [2008] and *Andrews and Forster* [2008] show that the spread may be greater still if rapid tropospheric adjustment processes are counted in the forcing, in an analogous way to stratospheric adjustment. For comparability with previous results, which likewise use a standard value for $F_{2\times}$, we ignore these issues here. Consequently the uncertainty in ρ may be underestimated (see also section 6).

[10] The regressions of decadal-mean F against ΔT in our set of AOGCMs give a 5–95% confidence interval for ρ of 2.0 ± 0.7 W m^{-2} K^{-1}, treating it as having a normal distribution (Table 1 and Figure 1). Since $F = \rho\Delta T$, the TCR can then be simply evaluated as $F_{2\times}/\rho$, the ΔT that corresponds to $F_{2\times}$. The model ρ range gives a TCR range of 1.4–2.6 K (median 1.8 K; the uncertainty is skewed because TCR $\propto 1/\rho$). The model TCR range evaluated by this method is not sensitive to the choice of $F_{2\times}$, because $F_{2\times}$ is used first to compute F and then to convert ρ to TCR, and these appearances of $F_{2\times}$ cancel each other.

[11] The TCR range calculated from ρ is of course similar to the actual range of ΔT at the time of 2 × CO_2 i.e., the definition of TCR. From the TCR values given by *Randall et al.* [2007] for our set of models, we consequently obtain almost the same range of ρ (Table 1).

2.2. Climate Feedback and Ocean Heat Uptake

[12] *Raper et al.* [2002] calculated α and κ for an earlier set of AOGCMs using the means of F, N and ΔT over years 61–80 of 1% CO_2 experiments, i.e., as $\alpha = (F - N)/\Delta T$ and $\kappa = N/\Delta T$. *Dufresne and Bony* [2008] have recently done the same for the CMIP3 AOGCMs. Here we evaluate them by OLS regression of decadal-mean F–N and N respectively against ΔT, as for ρ. The results for α and κ are shown in Table 1 and Figure 1. The 5–95% ranges are 1.4 ± 0.6 and 0.6 ± 0.2 W m^{-2} K^{-1} respectively, treating them as normal distributions. There is a tendency for our α to be larger and κ smaller than in the results of *Dufresne and Bony* [2008]. This is caused by the "cold start" effect in the 1% runs [*Hasselmann et al.*, 1993; *Keen and Murphy*, 1997], which means the regression of N against ΔT tends to have a small positive intercept, and a smaller slope than a line drawn from the origin to the point of 2 × CO_2 i.e., the ratio $N/\Delta T$ used by *Dufresne and Bony* [2008]. The difference thus reflects the fact that $N \propto \Delta T$ is not exact.

[13] These figures show that on average climate feedback is about twice the size of ocean heat uptake, but the relative

Table 1. Climate Feedback Parameter α, Ocean Heat Uptake Efficiency κ, and Climate Resistance ρ (All in W m^{-2} K^{-1}) Calculated by OLS Regression of Decadal-Mean $F - N$, N, and F Respectively Against ΔT Under a Scenario of CO_2 Increasing at 1% per Year for 70 Years in a Set of AOGCMs[a]

	Regression			AR4	D&B		
Model	α	κ	ρ	ρ	α	κ	$\Delta T_2/\Delta T_1$
CCSM3	1.84	0.67	2.51	2.5	–	–	1.3
CGCM3.1(T47)	1.28	0.55	1.83	1.9	–	–	1.3
CNRM-CM3	1.60	0.58	2.18	2.3	1.2	0.8	1.3
CSIRO-Mk3.0	1.60	0.83	2.44	2.6	–	–	–
ECHAM/MPI-OM	1.01	0.66	1.67	1.7	0.9	0.6	1.5
GFDL-CM2.0	1.96	0.64	2.60	2.3	1.2	0.5	1.5
GFDL-CM2.1	1.74	0.73	2.48	2.5	1.4	0.8	1.4
GISS-EH	1.46	0.77	2.23	2.3	–	–	–
INM-CM3.0	1.77	0.48	2.24	2.3	1.5	0.6	1.5
IPSL-CM4	1.03	0.70	1.73	1.8	1.0	0.8	1.3
MIROC3.2(hires)	0.87	0.56	1.43	1.4	–	–	–
MIROC3.2(medres)	0.97	0.81	1.77	1.8	0.9	0.8	1.4
MRI-CGCM2.3.2	1.23	0.41	1.63	1.7	1.5	0.6	1.1
PCM	2.08	0.45	2.52	2.8	1.5	0.6	1.1
UKMO-HadCM3	1.09	0.53	1.62	1.9	1.0	0.6	–
UKMO-HadGEM1	1.27	0.56	1.87	1.9	–	–	1.3
Ensemble	1.4 ± 0.6	0.6 ± 0.2	2.0 ± 0.7	2.1 ± 0.7			

[a]The uncertainties in the "Ensemble" row are the 5–95% range assuming a normal distribution for the models. The results are compared with ρ calculated as $F_{2\times}$/TCR from the values of TCR in Table 8.2 of *Randall et al.* [2007], and α and κ from *Dufresne and Bony* [2008]. $\Delta T_2/\Delta T_1$ is the ratio of the warming over the second 70 years to the warming over the first 70 years as the 1% increase of CO_2 continues (see section 6 for details).

importance of α and κ varies among models. In some (e.g., PCM) ocean heat uptake is much smaller than climate feedback, while in others (e.g., MIROC3.2, both resolutions) they are comparable. If α and κ are both constant, the realized warming ΔT at any time in a given model is a constant fraction of the equilibrium warming ΔT_{eqm} for the forcing, since $F = \alpha \Delta T_{eqm} \Rightarrow \Delta T/\Delta T_{eqm} = \alpha/(\alpha + \kappa)$. Models with a larger κ have a smaller realized fraction of warming at any time.

[14] *Raper et al.* [2002] found that in the set of models they considered there was an anticorrelation between α and κ; large equilibrium climate sensitivity (small α) tended to go with large ocean heat uptake efficiency (large κ). This tendency meant that the range of TCR was smaller than if the two factors had been independent, and they tentatively suggested physical mechanisms which might be responsible. In the CMIP3 models, however, this tendency is absent, as noted also by *Plattner et al.* [2008]. The correlation coefficient between α and κ across the CMIP3 models is −0.1, not significantly different from zero.

3. Climate Resistance From Simulated Past Changes

[15] The previous section shows that constant ρ is a good approximation in the idealized 1% CO_2 scenario up to 2 × CO_2, but that there is a large model uncertainty in ρ. We wish to consider whether ρ can be evaluated from past

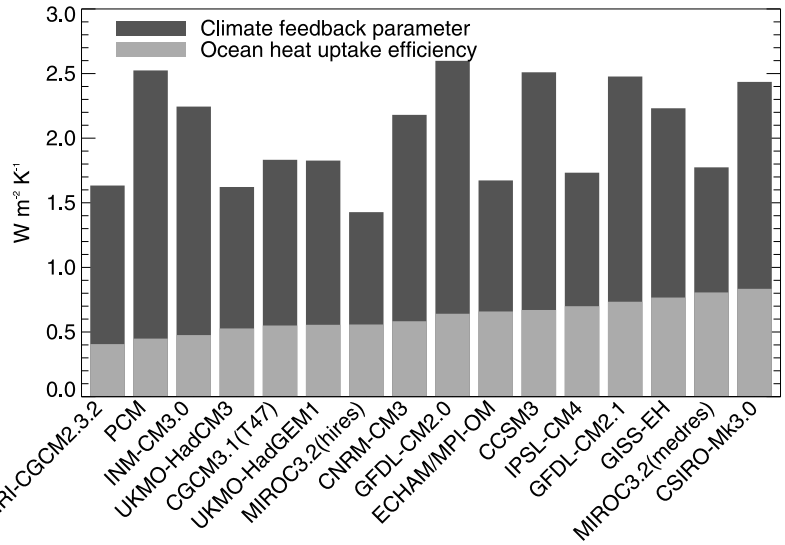

Figure 1. Climate feedback parameter α and ocean heat uptake efficiency κ in a set of 16 AOGCMs, from Table 1. The total height of each bar is the climate resistance $\rho = \alpha + \kappa$. The models are arranged in order of incre .

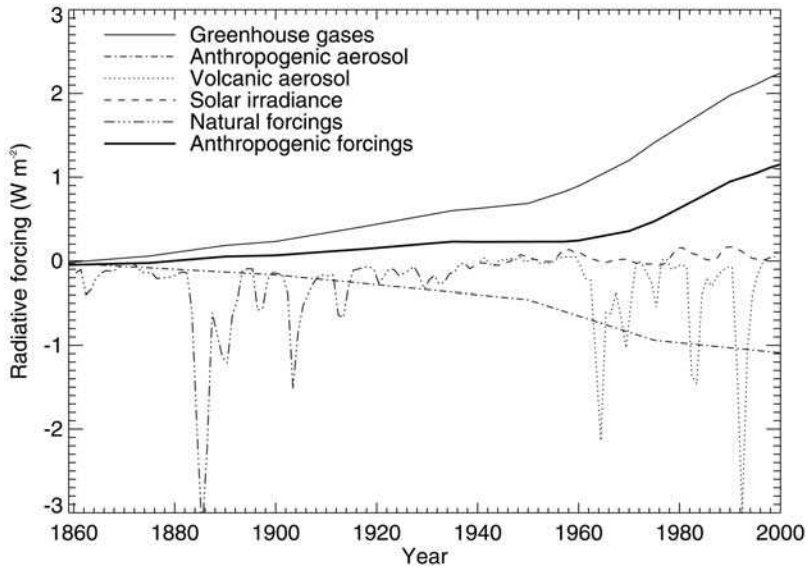

Figure 2. Radiative forcings in HadCM3 relative to its steady state control climate. Anthropogenic forcing is the sum of forcings from greenhouse gases and anthropogenic aerosol. Before 1940 the sum of volcanic and solar forcings (i.e., natural forcings) is shown because they were not separately diagnosed.

climate change. In this section we evaluate the climate resistance from simulations of the last 150 years carried out with the HadCM3 AOGCM [*Gordon et al.*, 2000], in order to test whether ρ thus obtained is consistent with the results of the HadCM3 1% CO_2 experiment.

[16] Both temperature change ΔT and radiative forcing F are defined relative to a steady state climate in which the forcing agents are constant. In AOGCM simulations of recent climate change, this unperturbed climate is often taken to be the late nineteenth century. However, if we suppose that the perturbations are small enough to be treated as linear (an assumption that is implicit in the use of a constant ρ) we do not need to know the steady state in order to evaluate ρ, which depends only on the slope of F against ΔT and is unaffected by constant offsets [cf. *Gregory et al.*, 2002; *Forster and Gregory*, 2006].

3.1. Radiative Forcing

[17] The main radiative forcing agents of recent climate change are the following. Greenhouse gases (carbon dioxide, methane, nitrous oxide, halocarbons and ozone) make the largest contribution. Anthropogenic aerosol (the albedo and cloud effects of sulfate aerosol and black carbon) has a net negative forcing, offsetting a substantial part of the positive greenhouse-gas forcing. Volcanic aerosol has an episodically large negative forcing, following explosive eruptions, such as those of Krakatau (1883), Agung (1963), El Chichon (1982) and Pinatubo (1991); after each, it decays over a few years as the aerosol settles out of the stratosphere. Solar irradiance varies with the 11-year cycle, but has rather small longer term trends.

[18] Time series of these radiative forcings as used in HadCM3 simulations of the past are shown in Figure 2. (HadCM3 does not simulate the forcing due to black carbon aerosol.) These forcings are consistent within uncertainties with the current best estimates for the real world (section 4). When all forcings are included in the model, the simulated ΔT follows observations remarkably well [*Stott et al.*, 2000]. The relative influences of these forcings upon twentieth-century climate change has been studied in great detail by many workers on detection and attribution of climate change [e.g., *IDAG*, 2005] using AOGCM experiments like those with HadCM3, leading to the conclusion that "greenhouse gas forcing has very likely caused most of the observed global warming over the last 50 years" [*Hegerl et al.*, 2007].

3.2. Simulations With Anthropogenic Forcing Only

[19] We first consider the results from an ensemble of four experiments with anthropogenic forcing only F_{GA} i.e., greenhouse-gas and aerosol [*Stott et al.*, 2000]. (In the next subsection we consider natural forcing as well i.e., volcanic and solar.) We obtain ρ by regressing ΔT_{GA} against F_{GA}. This assumes there is no uncertainty in the values of F; the best fit slope is the one which minimizes the RMS deviation in ΔT of the data points from the regression line. This is appropriate because the forcing in the model is precisely known and effectively prescribed as a function of time. On the other hand, there is scatter in ΔT, due to unforced internal variability of the climate system, for example variability in cloudiness leading to fluctuations in absorbed shortwave radiation, or variation in oceanic upwelling affecting SSTs. By such mechanisms random variability is added to ΔT and N in the heat balance Equation 1, causing deviations from $\Delta T \propto F$. Whereas in the analysis of the 1% experiments, it was immaterial whether we chose ΔT or F as an independent variable, in these historical experiments the signal is weaker and the correlation lower, so the choice affects the results. This is consistent with the finding of *Spencer and Braswell* [2008], who use a simple model to illustrate how climate sensitivity can be biased high when diagnosed by linear regression under a small-forcing regime.

Table 2. Results for Correlation Coefficient r and Climate Resistance ρ (W m^{-2} K^{-1}) for Various Time Periods in the HadCM3 AOGCM Experiment Ensembles up to 1999 and the Real World up to 2006[a]

	1900–1999/2006		1970–1999/2006		1980–1999/2006	
	r	ρ	r	ρ	r	ρ
			HadCM3 Model			
T_{GA} *v* F_{GA} e-members	0.82	1.6 ± 0.2	0.82	1.6 ± 0.5	0.69	1.4 ± 0.6
T_{GA} *v* F_{GA} e-mean	0.94	1.6 ± 0.1	0.96	1.5 ± 0.1	0.91	1.4 ± 0.2
T_{all} *v* F_{GA} e-members	0.77	1.8 ± 0.2	0.83	1.5 ± 0.5	0.72	1.6 ± 1.3
T_{all} *v* F_{GA} e-mean	0.87	1.7 ± 0.2	0.95	1.5 ± 0.2	0.89	1.4 ± 0.3
b_F/b_T e-members	–	–	0.77	1.8 ± 0.6	0.63	1.9 ± 1.4
b_F/b_T e-mean	–	–	0.89	1.8 + 0.4–0.4	0.77	1.7 + 1.0–0.7
			Real World			
T *v* F_{GA}	0.80	1.7 + 0.3–0.2	0.90	2.1 + 0.4–0.3	0.84	2.1 + 0.8–0.4
T *v* F_G	0.86	3.2 + 0.4–0.3	0.91	2.2 + 0.4–0.3	0.85	2.0 + 0.7–0.4
Real b_F/b_T	–	–	0.91	2.5 + 0.5–0.4	0.84	2.9 + 1.2–0.8

[a]The lines with a title containing "T *v* F" show ρ from ordinary least squares regression of surface air temperature anomaly ΔT against radiative forcing F. Various estimates of ΔT and F are used, as described in the text. The lines with a title containing b_F/b_T show ρ calculated as the ratio of the rates of change of F and ΔT. For the model, the "e-members" lines show the mean r and the distribution of ρ calculated from the ΔT time series of the individual ensemble members, while the "e-mean" lines show r and ρ calculated from the ensemble-mean ΔT time series. Uncertainties are 5–95% confidence intervals: $a + b - c$ means the median is a, 95-percentile $a + b$ and 5-percentile $a - c$.

[20] We evaluate ρ for each of the four HadCM3 ensemble members for three time periods. (These model integrations end in 1999.) We calculate the ensemble average and spread of the results (shown as "T_{GA} *v* F_{GA} e-members" in Table 2). The use of an ensemble allows us to quantify the uncertainty which arises from internally generated (unforced) variability on all timescales. The influence of unforced variability can be reduced by calculating the ensemble-mean $\Delta T_{GA}(t)$ year-by-year, and regressing this time series against F_{GA} ("e-mean" in Table 2, shown in Figure 3). Because the signal-to-noise ratio is higher in the ensemble-mean time series, the correlation coefficients are higher for e-mean than for e-members. The standard deviation of unforced variability in ΔT estimated from the residuals about regression line is about the 0.12 K for the ensemble members, and 0.06 K for the ensemble mean i.e., smaller by $\sqrt{4}$, as we would expect.

[21] Similarly, the uncertainties on ρ are larger for shorter periods because the forced climate change is relatively smaller compared with the unforced variability. Autocorrelation in the time series would lead to an underestimate of the uncertainty in ρ, but there is insignificant autocorrelation in the deviations of ΔT_{GA} from a linear trend against time. Within their uncertainties, all the regressions give values of ρ which are consistent with 1.6 ± 0.1 Wm^{-2} K^{-1} obtained from the HadCM3 1% CO_2 experiment (Table 1).

3.3. Simulations With Both Anthropogenic and Natural Forcing

[22] We now consider the results from an ensemble of four HadCM3 experiments with forcing F_{all} from both anthropogenic and natural factors [*Stott et al.*, 2000]. On examining the plot of ΔT_{all} against F_{all}, the sum of anthropogenic and natural forcing, we find that a few years

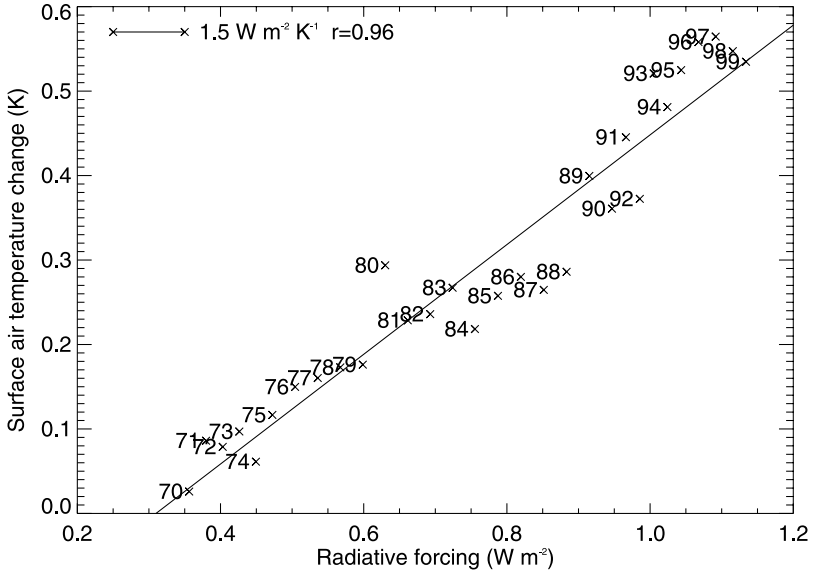

Figure 3. Annual mean surface air temperature anomaly ΔT_{GA} from the ensemble-mean of HadCM3 anthropogenic-forcings experiments plotted against anthropogenic radiative forcing F_{GA}. Each point is labeled with it . The line is obtained by ordinary least squares regression of ΔT_{GA} against F_{GA}.

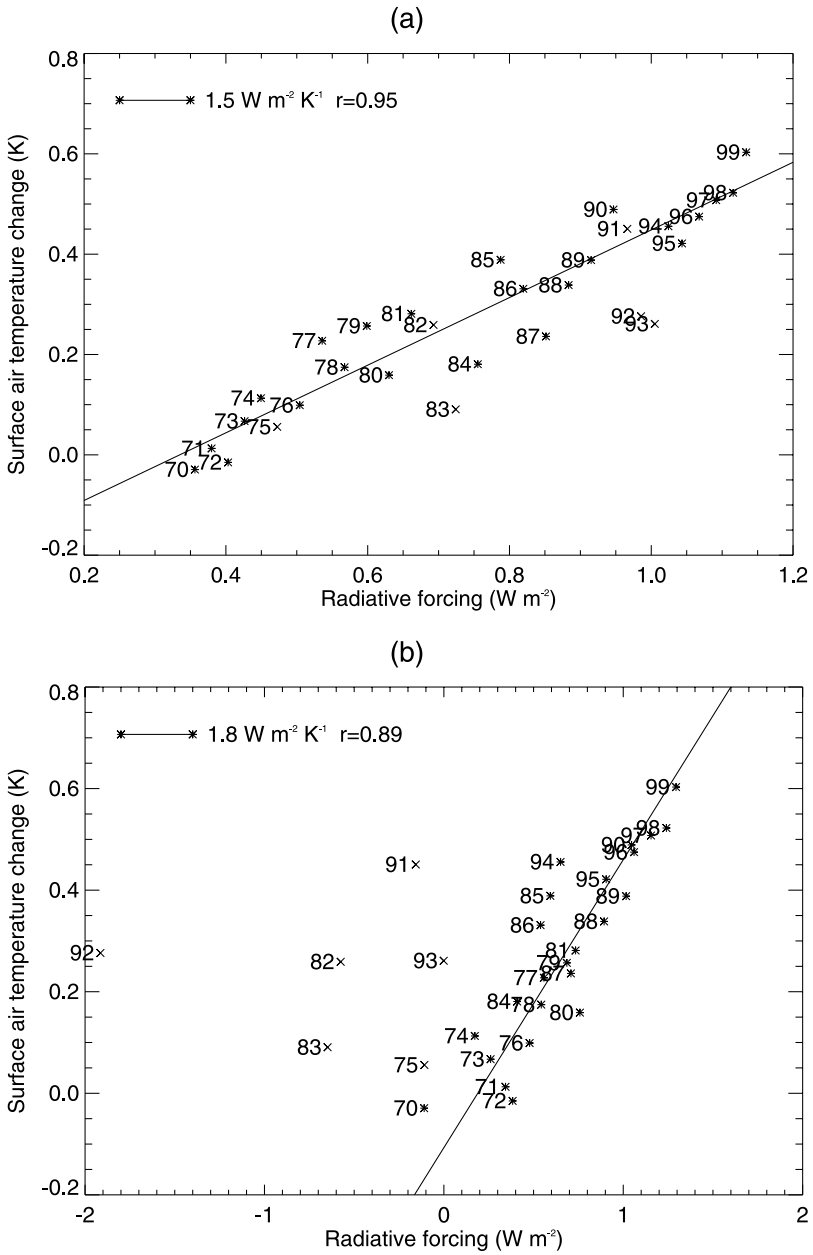

Figure 4. Relationship between annual-mean radiative forcing and surface air temperature anomaly ΔT_{all} from the ensemble mean of the HadCM3 all-forcings experiments for 1970–1999. Each point is labeled with its year. (a) ΔT_{all} is plotted against anthropogenic forcing F_{GA}. The line is obtained by ordinary least squares regression of ΔT_{GA} against F_{GA} (the first method in the text). (b) ΔT_{all} is plotted against the sum of radiative forcings F_{all}. The line is obtained by ordinary least squares regression of ΔT_{all} and F_{all} separately against time (the second method in the text). In both cases the fits excluded years strongly affected by volcanoes, which are those indicated by crosses; those included in the fits are indicated by asterisks.

lie substantially to the left of the regression line which fits the majority of years i.e., they are at higher ΔT or lower F_{all} than expected (Figure 4b). The correlation of the ensemble-mean ΔT_{all} with F_{all} is only 0.41. The deviant years are ones soon after a large volcanic eruption. The response of ΔT to the episodic volcanic forcing is much weaker than its response to the decadal increase in total forcing. We suppose this is because the rapid response of ocean heat content to the sudden negative forci m a volcano is different in character from its response to the slower changes caused by other kinds of forcing [*Forster and Collins*, 2004; *Forster and Gregory*, 2006; *Hegerl et al.*, 2007]. Consideration of vertical heat transport and heat capacity is necessary to model it correctly. Consequently the climate response to volcanoes cannot be described by the same relationship $F = \rho\Delta T$ as multidecadal climate change; either the climate resistance ρ is not the same as for decadal timescales or a relationship of this form is inapplicable.

[23] Since our interest is in the longer timescales, we exclude the years strongly affected by volcanoes (the "volcano" years) from the calculation, identifying them as those in which the volcanic forcing has a magnitude exceeding 0.5 W m^{-2}. This is an ad-hoc criterion to remove the points that lie far off a linear relationship. However, the volcanic forcing is not zero in the other years. To obtain an estimate of ρ under these circumstances, we have tried three methods, in all cases excluding the volcano years.

3.3.1. Ordinary Least Squares Regression of ΔT_{all} Against F_{GA}

[24] The first method is to disregard the natural forcing altogether, and regress ΔT_{all} against the anthropogenic forcing F_{GA} as before (Figure 4a and "Model T_{all} *v* F_{GA}" in Table 2). We treat the solar forcing like the volcanic because its dominant variation is likewise not monotonic, but periodic, on the 11-year solar cycle. We assume that such forcings do not affect ΔT on decadal timescales. The results of the regression are not significantly different from those using T_{GA}, because in these HadCM3 experiments the overall warming in the 20th century, and its trend since 1970, are similar with and without natural forcing [see *Gregory et al.*, 2006, their Figure 2], consistent with the assumption that natural forcings have little long-term effect. This is not surprising given their small average magnitude and trends (Figure 2). The standard deviation of unforced variability estimated from the residuals is about 0.12 K, as from the regression against F_{GA}. This equals the interannual standard deviation of ΔT in the HadCM3 control run, in which forcing is constant, so only the unforced internal variability is present. The equality indicates that short-period fluctuation in the natural forcing has little effect on ΔT.

3.3.2. Ratio of Rates of Change of ΔT_{all} and F_{all}

[25] The second method takes natural forcing into account but assumes that it affects only the trend in ΔT, not its interannual fluctuations. This method makes use of additional information about time-dependence, which is not exploited by regression. During recent decades, excluding the volcano years, the time series of both ΔT and F_{all} can be reasonably well fitted by linear functions of time t i.e., $\Delta T = a_T + b_T t$ and $F_{all} = a_F + b_F t$. For 1970–1999, the correlation coefficients with time of ΔT in individual experiments are 0.8–0.9, of ensemble-mean ΔT 0.95, and of F_{all} 0.88. Linear time-dependence is not a good approximation for the twentieth century as a whole, so we do not use this method for the entire period. The coefficients of the time-dependence can be estimated by OLS regression, because the independent variable in each case is time, in which there is no uncertainty. If both F_{all} and ΔT depend linearly on time, they must have a linear relationship with each other:

$$F_{all} = a_F + b_F t = a_F + b_F(\Delta T - a_T)/b_T$$
$$= (a_F - a_T b_F/b_T) + (b_F/b_T)\Delta T,$$

i.e., the linear relationship implied between F_{all} and ΔT has slope $\rho = b_F/b_T$, the ratio of the rates of change of F_{all} and ΔT (Figure 4b, and "Model b_F/b_T" in Table 2).

[26] The results for ρ from this rate-ratio method (1.8 + 0.4–0.4 W m^{-2} K^{-1} for the ensemble mean in 1970–1999) are larger than from the OLS regression. This is because of the difference in the forcing time series, not the different method. If we apply the rate–ratio method to obtain ρ from ΔT_{all} and F_{GA}, we obtain the same results as we did by OLS regression of ΔT_{all} against F_{GA}. It arises because F_{all} has a greater upward trend than F_{GA}, owing (in the HadCM3 time series) to an increase in solar forcing in the 1970s, and an increase in volcanic forcing i.e., a reduction in negative forcing in the late 1990s. Note that this increase comes only from the years with weak or no volcanic forcing, since the years strongly affected by volcanoes have been entirely excluded, possibly giving a biased estimate of the natural forcing trend.

[27] The uncertainty on ρ is estimated using a Monte Carlo technique with the uncertainties on b_T and b_F from the separate regressions. (Because b_F/b_T is nonlinear in b_T, the confidence interval is not symmetrical.) The uncertainty is larger than from the OLS regression against F_{GA} (the first method) because the short-period fluctuations in F_{all} make its trend b_F relatively uncertain. If these fluctuations have an effect on T_{all}, part of the uncertainty in b_T is correlated with uncertainty in b_F; ignoring this means the uncertainty in their ratio is overestimated. However, the evidence from the first method is that such an effect must be small.

3.3.3. Total Least Squares Regression of ΔT_{all} Against F_{all}

[28] Because of the fluctuations in F_{all}, we cannot use what might appear to be the obvious method of OLS regression of T_{all} against F_{all}. The fluctuations represent an uncertainty in F_{all}, which means that OLS regression is inapplicable [cf. *Spencer and Braswell*, 2008], as it assumes there is no uncertainty in the independent variable. Given an *a priori* estimate of this uncertainty, we could use the modified method, called "total least squares regression" (TLS) by workers in optimal climate fingerprinting, which allows for uncertainty in both variables. We have tried this method too, employing software from the Goddard Space Flight Center IDL Astronomy User's Library that implements the algorithm described by *Press et al.* [1992, their section 15.3 on straight line data with errors in both coordinates]. As estimates of the independent uncertainties in T_{all} and F_{all}, we used the standard deviations derived from the residuals in their separate regressions of T_{all} and F_{all} against time.

[29] This TLS method gives very similar results (not shown) to the rate–ratio method (in fact they are the same for 1970–1999 to one decimal place), but it involves additional assumptions that are doubtful. First, it assumes that the same relation $F_{all} = \rho \Delta T_{all}$ applies to interannual variability as to the longer-term trend; this is certainly not the case in the volcano years, and may not be correct for other years, given the lack of evidence for correlation of interannual variability between T_{all} and F_{all}. Second, it assumes that the uncertainty in F_{all} is normally distributed, which is not true because the volcanic forcing has a skewed distribution, with a longer negative tail. Because these reservations make the TLS method less robust, without yielding a reduction in uncertainty in the results, we prefer the rate-ratio method to the TLS method.

3.4. Summary of Results From HadCM3 Simulations of the Past

[30] From the HadCM3 results, we conclude that the climate resistance is not significantly different for historical

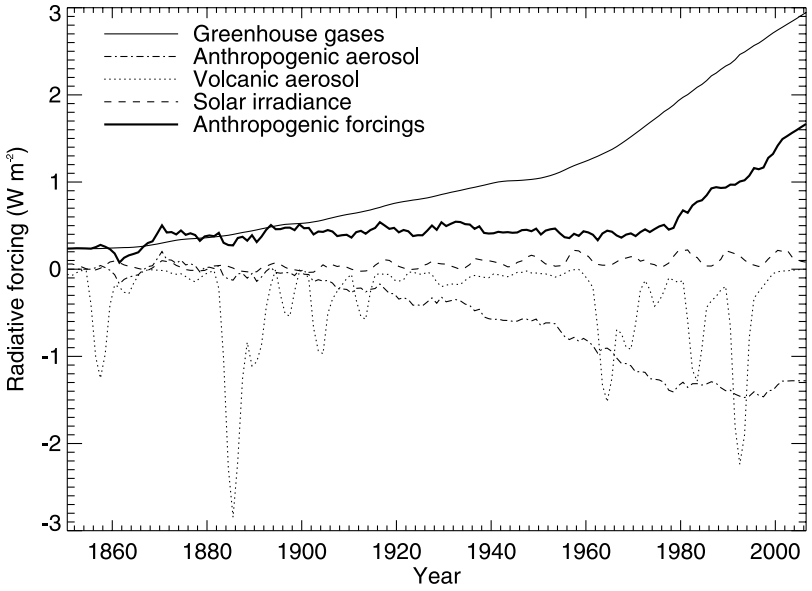

Figure 5. Median estimates of real-world radiative forcings relative to 1850. Anthropogenic forcing is the sum of forcings from greenhouse gases and anthropogenic aerosol.

anthropogenic forcing in the twentieth century and for the idealized future 1% increase of CO_2 from which TCR is evaluated. It is obvious that the strong but short-lived forcing from volcanoes does not affect ΔT in the same way as anthropogenic forcing, but it is unclear what effect natural forcings have on the trend of ΔT. If we assume that their trend on multidecadal timescales affects the trend of ΔT, the climate resistance accounting for natural forcing in recent decades but excluding years with strong volcanic forcing is about 20% higher than for anthropogenic forcing alone (i.e., the ratio of ρ with natural forcing included to ρ without taking natural forcing into account). However, the exclusion of volcano years may bias this result. We therefore prefer the estimate without natural forcing, but note this issue as a systematic uncertainty.

4. Climate Resistance From Observed Past Changes

[31] Having shown that the TCR of HadCM3 can be evaluated from its simulation of past changes, we next apply the same methods to estimates of past changes in the real world. Global average surface air temperature change during the last century is a relatively well-observed quantity. We use the time series derived by the Met Office and the University of East Anglia [HadCRUT3; *Brohan et al.*, 2006]. As well as the scatter due to internal climatic variability, individual years have some random measurement and sampling error. In recent decades this has a standard deviation of 0.037 K [*Brohan et al.*, 2006, their Figure 12].

[32] Estimates of past radiative forcing have considerable uncertainty, despite improvements in recent years [*Forster et al.*, 2007]. We show time series in Figure 5 of median estimates of the forcings. Long-lived greenhouse-gas forcings are derived from ice core, firn and in-situ measurements from a variety of sources [see *Forster et al.*, 2007]. Solar forcings are by *Wang* [2005]. Aerosol forcings are derived from the HadGEM1 AOGCM by *Forster and Taylor* [2006] and include a component due to land-use changes. The HadGEM1 model was chosen as it included absorbing aerosol species and its total aerosol forcing in 2005 matched the best estimate of the IPCC WG1 AR4 [see *Forster et al.*, 2007]. Volcanic and ozone forcings are by *Myhre et al.* [2001], scaled to match the IPCC WG1 AR4 estimate in 2005, assuming no change in forcing during 2000–2005.

4.1. Climate Resistance From OLS and Rate-Ratio Methods

[33] The uncertainty in the anthropogenic forcing is systematic, i.e., it means that any of the terms might be *consistently* over- or underestimated, rather implying random errors in individual years. Hence, as in the model, we can use OLS regression of ΔT against F_{GA}, which implicitly assumes a uniform prior distribution for the dependent variable ΔT, i.e., all values are equiprobable in the absence of knowledge. Since the purpose is to evaluate ΔT for a given forcing, this choice of prior is consistent with the suggestion of *Frame et al.* [2005].

[34] Excluding years strongly affected by volcanoes by the same criterion as in the model, we evaluate ρ for the three time periods (Figure 6a, and "Real T v F_{GA}" in Table 2). For recent decades, ρ in the real world ($2.1 + 0.4 - 0.3$ W m^{-2} K^{-1} for 1970–2006) is a little larger than in HadCM3. (The uncertainty is not symmetrical because ρ is the reciprocal of the regression slope.) The correlation coefficients are high, and the statistical uncertainties on ρ are smaller for longer time periods.

[35] As in the model, we compare this with ρ from the ratio of the slopes of F_{all} and T, excluding volcano years, separately regressed against time, in order to take into account the trend of the natural forcing (Figure 6b, and "Real b_F/b_T" in Table 2). Again, as in the model, the resistance from this method ($2.5 + 0.5 - 0.4$ W m^{-2} K^{-1} for 1970–2006) is larger than from OLS regression of ΔT

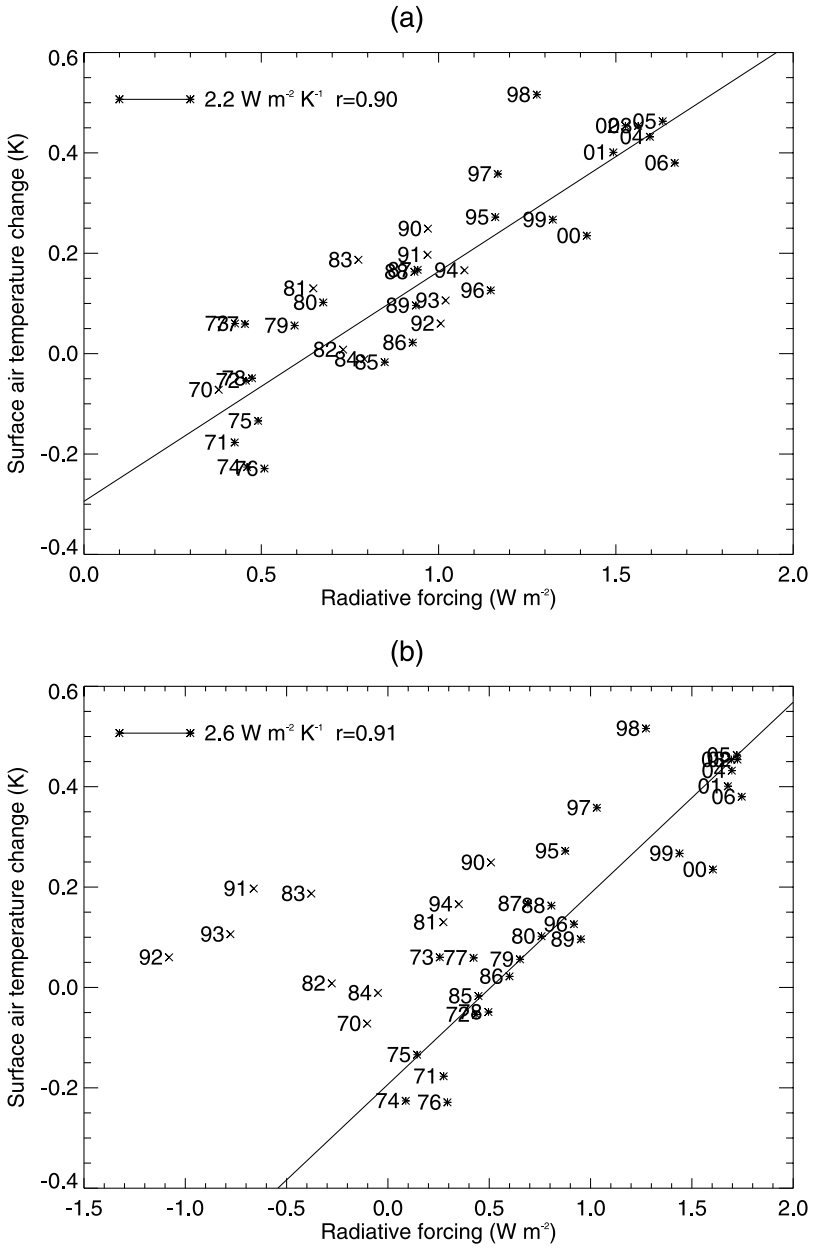

Figure 6. Relationship between annual-mean estimated real-world radiative forcing and observed surface air temperature anomaly ΔT for 1970–2006. Each point is labeled with its year. (a) ΔT is plotted against anthropogenic forcing F_{GA}. The line is obtained by ordinary least squares regression of ΔT against F_{GA} (the first method in the text). (b) ΔT is plotted against the sum of radiative forcings F_{all}. The line is obtained by ordinary least squares regression of ΔT and F_{all} separately against time (the rate-ratio method, the second method in the text). In both cases the fits excluded years strongly affected by volcanoes, which are those indicated by crosses; those included in the fits are indicated by asterisks.

against F_{GA}, which we prefer, for reasons summarized in section 3.4.

4.2. Uncertainty From Forcing

[36] The systematic uncertainty in F_{GA} gives rise to systematic uncertainty in ρ in addition to the statistical uncertainty from unforced variability. The largest systematic uncertainty in F_{GA} is associated with the poorly known anthropogenic aerosol forcing F_A. During the twentieth century as a whole F_A is temporally anticorrelated with the greenhouse-gas forcing F_G (Figure 5). If we underestimate the magnitude of F_A, we will overestimate the increasing tendency of $F_G + F_A$, which will reduce the fitted slope in the regression of ΔT versus F_{GA}, and hence bias ρ upward. Fingerprinting studies can distinguish better between the effects of F_G and F_A by considering the spatial patterns than we can do here by using only global averages [*Stott et al.*, 2006].

[37] We can minimize the influence of the uncertainty in F_A by considering a period when it is changing least rapidly

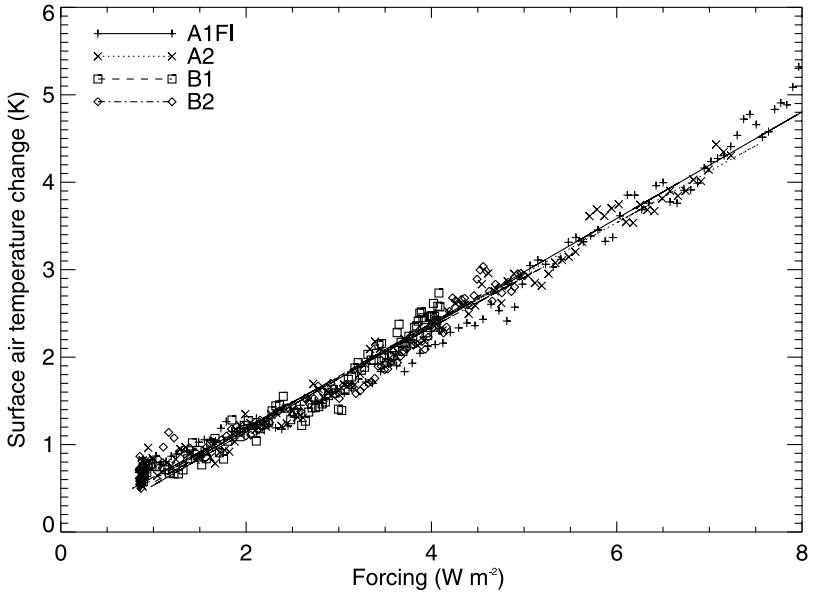

Figure 7. Annual-mean global-mean surface air temperature change ΔT and radiative forcing F, with respect to steady state in the late nineteenth century, simulated for the twenty-first century using the HadCM3 AOGCM under the four SRES marker scenarios indicated. For each scenario, a regression line has been plotted.

[*Forster and Gregory*, 2006]. That suggests restricting our attention to recent decades [*Myhre et al.*, 2001, and Figure 5]. In Table 2 we show the results of regression against F_G ("Real T *v* F_G"). The comparison with the results for F_{GA} confirms that omitting F_A leads to larger ρ for 1900–2006, during which period F_A changed substantially, but that results for 1970–2006 and 1980–2006 are insensitive to F_A. Henceforth, we prefer to use 1970–2006 rather than 1980–2006 since the longer of these periods gives smaller statistical uncertainty in ρ. *Forster et al.* [2007] give a median estimate of $F_A = -1.3$ W m^{-2} at 2005, with a 5–95% range of -0.5 to -2.2 W m^{-2}. If we assume the fractional uncertainty to be time-independent and scale $F_A(t)$ by factors within this range, ρ for 1970–2006 is unaffected to two significant figures. Consequently we do not include an allowance for aerosol uncertainty in our results. However, we note that any time-dependent bias in the aerosol forcing would introduce a systematic error in ρ.

[38] Most of F_G is due to long-lived greenhouse gases, whose forcing has an uncertainty of 10% [*Forster et al.*, 2007, their Table 2.12]. Forcing by ozone, both tropospheric and stratospheric, is smaller, but with a larger fractional uncertainty. During the twentieth century, ozone forcing was a reasonably constant fraction (9–14%) of F_G. Therefore we account for the ozone forcing uncertainty as a constant fraction of F_G, and we estimate that it increases the uncertainty on F_G to 13%, by reference to *Forster et al.* [2007]. We combine this 13% systematic uncertainty on ρ with the statistical uncertainty on ρ from the OLS regression, and obtain $\rho = 2.1 + 0.5–0.4$ W m^{-2} K^{-1} (for 1970–2006).

[39] Since uncertainty in F_A is disregarded, and uncertainty in F_G is common to $F_{2\times}$ and ρ, we can omit forcing uncertainty in converting ρ to TCR. Our $\rho = 2.1 + 0.4 - 0.3$ W m^{-2} K^{-1} implies a 5–95% range for TCR $= F_{2\times}/\rho$ in the real world of 1.5–2.1 K. This range is narrower than and lies within CMIP3 range of 1.2–2.4 K [*Meehl et al.*, 2007].

4.3. Effect of Longer-Period Unforced Variability

[40] The statistical uncertainty on the slope from OLS regression of ΔT against F_{GA} reflects the effect of unforced variability on ΔT on timescales which can be adequately sampled by the length of the time series used. However, unforced variability on longer timescales is not included. For instance, some or all of the trend in ΔT during 1970–2006 might be due to internally generated climate variability on multidecadal timescales, rather than being caused by the forcing. This is the reason why the uncertainty from the ensemble mean in section 3 (Table 2) is greater than from the ensemble members, which have a spread arising from longer-period unforced variability. We cannot assess such variability from the observed ΔT, since we have only one realization of the real world. This problem is related to that of "detection" of climate change, i.e., deciding statistically whether the observed ΔT time series is consistent with unforced variability. It becomes more severe the shorter the observational record used, because the unforced variability becomes relatively larger. For example, *Chylek et al.* [2007] evaluate α from ΔT over the last decade by assuming it is entirely a forced response; we suggest that there is substantial uncertainty in the results from such a short period due to unforced variability.

[41] This problem can only be addressed quantitatively by using AOGCM control runs to assess the effect of variability on longer timescales. To do this, we use ΔT reconstructed from the OLS regression line of observed ΔT against F_{GA}, i.e., remove the temporal variability, generate a set of realizations with synthetic temporal variability by adding randomly selected portions from CMIP3 AOGCM control runs to the reconstructed time series, and evaluate

the distribution of ρ from fitting the realizations. We carried out this procedure using 19 different control runs. We also included randomly generated synthetic measurement and sampling uncertainty of the size estimated for the HadCRUT3 ΔT time series, but this has negligible effect by comparison with the variability from the control runs. The TCR range estimated from the real world is widened by allowing for this longer-period variability. However, the AOGCMs differ considerably regarding the magnitude of the effect. For instance, for standard deviations of trends over a period of the length of 1970–2006, CCCma CGCM3.1(T47) has 0.14 K century^{-1}, UKMO-HadCM3 0.30 and GFDL-CM2.1 0.49. In these cases, the TCR range is 1.5–2.1 K (not significantly widened), 1.3–2.3 K and 1.1–2.4 K respectively. It is notable that the last two are similar to the CMIP3 range, and that the means of both CMIP3 and our ranges are 1.8 K.

5. TCR and Equilibrium Climate Sensitivity

[42] The equilibrium climate sensitivity $\Delta T_{2\times} = F_{2\times}/\alpha$ is the warming in a steady state under $2\times CO_2$, as discussed in section 1. *Meehl et al.* [2007] report that the 5–95% range of equilibrium climate sensitivity in CMIP3 models is 2.1–4.4 K. Over the last three decades, a lot of attention has been given to $\Delta T_{2\times}$ but it is still relatively poorly constrained. A number of studies examined by *Hegerl et al.* [2007] and summarized by *Meehl et al.* [2007] (Box 10.2) have set observational constraints, but these are fairly weak, especially on the upper bound. That raises the question of why our observational constraint on the TCR is by contrast rather strong.

[43] Observational estimates of $\Delta T_{2\times}$ are, in effect, attempting to deduce the climate feedback parameter α from $\Delta T(t)$ in nonequilibrium states, when $\Delta T = F/(\alpha + \kappa)$ and $\alpha = (F - N)/\Delta T$. There are three reasons why uncertainty is larger in observational estimates of $\Delta T_{2\times}$ than in our estimate of TCR.

[44] First, F is poorly known. This is the dominant uncertainty if climate change relative to the preindustrial state is considered [*Gregory et al.*, 2002] because of the aerosol forcing uncertainty, to which we have limited our exposure by our choice of time period (section 3.3).

[45] Second, if $\Delta T_{2\times}$ is large and α small, such that $\alpha \ll \kappa$, then ΔT is insensitive to α. In this situation, $N \approx F$; the forcing is mostly being taken up by the ocean, climate feedback is making only a small contribution to resisting climate change, and it is hard to quantify α from this contribution. That is why the upper bound of $\Delta T_{2\times}$ is particularly uncertain. Another expression of this is the nonlinear relation between TCR and $\Delta T_{2\times}$:

$$\mathrm{TCR} = \frac{F_{2\times}}{\alpha + \kappa} = \frac{F_{2\times}}{(F_{2\times}/\Delta T_{2\times}) + \kappa} = \frac{\Delta T_{2\times}}{1 + (\kappa \Delta T_{2\times}/F_{2\times})}.$$

For small $\Delta T_{2\times}$, TCR$\simeq\Delta T_{2\times}$, but for $\Delta T_{2\times} \to \infty$, TCR $\to F_{2\times}/\kappa$, i.e., independent of $\Delta T_{2\times}$. This is illustrated from model results by *Knutti et al.* [2005, Figure 3a] and *Meehl et al.* [2007, Figure 10.25a], showing how TCR tends to level off for large $\Delta T_{2\times}$. For large $\Delta T_{2\times}$, even with a small uncertainty in TCR and ρ, there can be a large uncertainty in $\Delta T_{2\times}$ and α.

[46] Third, to extract α from $\alpha + \kappa$ requires a knowledge of N, to obtain κ. This can be evaluated from heat storage in the ocean [*Gregory et al.*, 2002; *Forest et al.*, 2006] or the TOA radiative flux [*Forster and Gregory*, 2006], but in either case it is rather uncertain from observations. Moreover, there is internal variability in N, as discussed in section 3.2, which increases the uncertainty in the evaluation of κ. When we evaluate $\rho = \alpha + \kappa$, however, we do not need a knowledge of N, because we are quantifying the overall climate response, rather than climate feedback or ocean heat uptake separately. Consistency with observed ΔT in effect requires some cancellation of uncertainty between α and κ [cf. *Knutti and Tomassini*, 2008].

6. Projections of Future Temperature Change

6.1. Scenario Dependence of Climate Resistance

[47] When we first introduced $\rho = \alpha + \kappa$, we remarked that we expected $F = \rho \Delta T$ with constant ρ only to apply for scenarios of fairly steadily increasing forcing, because the approximation of constant κ would otherwise be inadequate. Moreover, for scenarios with a slower rate of increase of F, the climate system at any time will be nearer the steady state $F = \alpha \Delta T$, so ρ will be smaller.

[48] We can test the approximation of a constant scenario-independent ρ for projections of the twenty-first century in simulations following various SRES emissions scenarios [*Nakićenović et al.*, 2000] made with HadCM3 [*Johns et al.*, 2003], using the ΔT and F diagnosed from the model. The SRES scenarios give a range of increase in F over the twenty-first century (figures from the simple climate model of *Cubasch et al.* [2001], Appendix II.3 of the report) which would be achieved by rates of CO_2 increase alone of between 0.5% and 1.5% compounded per year, bracketing the idealized 1% scenario. The HadCM3 experiments show a scenario-independent linear relationship between ΔT and F (Figure 7). The relationship is not perfect because of variability on all timescales generated internally by the climate system. Nonetheless, the correlation coefficients are at least 0.98. The climate resistance ρ obtained from OLS regression of ΔT against F is 1.6–1.8 W m^{-2} K^{-1}, depending a little on scenario, but similar to $\rho = 1.6 \pm 0.1$ W m^{-2} K^{-1} calculated from the 1% experiment.

[49] Unfortunately radiative forcings from SRES scenarios have not generally been diagnosed in AOGCMs, so we cannot present results similar to Figure 7 from other AOGCMs. *Forster and Taylor* [2006] estimated the forcing for SRES A1B in several models, but their method depends on the assumption that α in each model is constant in time and not affected by the scenario, so the results they obtain are not entirely independent of the hypothesis we wish to test.

[50] However, using CMIP3 results for a wider range of AOGCMs we can consider the ratio $R_{a/b} \equiv \Delta T_a(t)/\Delta T_b(t)$ for pairs of SRES scenarios a and b. If ρ is a constant, or depends only on time, in any given model $R_{a/b}(t) = F_a(t)/F_b(t)$. If different models use the same forcings $F_a(t)$ and $F_b(t)$, $R_{a/b}(t)$ will be model-independent. *Meehl et al.* [2007] tuned a simple climate model to replicate the results of 19 AOGCMs from the CMIP3 database for SRES scenarios B1, A1B and A2. For any pair of SRES scenarios, $R_{a/b}(t)$ is indeed very similar for the different tunings. For the pairs of

scenarios available from the AOGCMs, $R_{a/b}(t)$ has a substantial spread over models, which is likely to be due to model dependence in $F(t)$. However, the AOGCM-mean $R_{a/b}(t)$ is very close to $R_{a/b}(t)$ from the simple model, giving some evidence for the scenario independence of climate resistance. *Meehl et al.* [2007] and *Knutti et al.* [2008] used this finding to estimate the AOGCM-mean $\Delta T_a(t)$ for SRES scenarios for which the AOGCMs had not been run by scaling the AOGCM-mean ΔT_{A1B} according to $\Delta T_a(t) = \Delta T_{A1B}(t)\ R_{a/A1B}(t)$ with $R_{a/A1B}(t)$ from the simple climate model.

[51] *Stouffer and Manabe* [1999] carried out a set of experiments with the GFDL_R15_a AOGCM in which they applied rates of CO_2 increase of between 0.25% and 4% compounded per year, a much broader range than encompassed by the SRES scenarios. Although all their experiments exhibit good linear relationships (their Figure 5), they show a substantial scenario dependence in ρ (calculated from their Table 2), which varies between 1.4 W m^{-2} K^{-1} for 0.25% and 2.5 W m^{-2} K^{-1} for 4%. It is smaller for lower rates, as expected. However, its variation between the 1% scenario (1.7 W m^{-2} K^{-1}) and the 2% scenario (2.1 W m^{-2} K^{-1}) is only ±10%, while in HadCM3, the 2% scenario results in $\rho = 1.8 \pm 0.1$ W m^{-2} K^{-1}, only slightly larger than for the 1% scenario. Hence we consider that a scenario-independent ρ is an acceptable approximation for SRES and other scenarios of practical interest for the twenty-first century. During 1970–2006 the real-world anthropogenic forcing $F_{GA}(t)$ had a rate of increase equivalent to CO_2 alone rising at 0.7% compounded per year. Since this is within the SRES range, it supports the use of data from 1970–2006 to obtain a value for ρ appropriate for the twenty-first century.

6.2. Projections for SRES Scenarios Using Climate Resistance

[52] If $F = \rho\Delta T$ holds, we can use ρ to make projections of ΔT given F. For example, under emissions scenario SRES A1B the best estimate of the difference in F_G between 2095 and 1990 is +4.3 and in F_A +0.6 W m^{-2} (also positive because aerosol forcing is projected to become less negative during the century). We assume that the projections of the contributions to the forcing have the same fractional uncertainties as their present-day estimates, namely for F_G a normal distribution with a 5–95% range of ±13%, and for F_A following the probability density function from *Boucher and Haywood* [2001], *Haywood and Schulz* [2007] and *Forster et al.* [2007]. Combining these by Monte Carlo sampling gives a 5–95% range of 4.4–5.5 W m^{-2} for F_{GA}.

[53] Again using a Monte Carlo, we calculate F_{GA}/ρ with ρ from the OLS regression in section 4. The uncertainty on ρ includes a contribution from the systematic uncertainty in past F_G, which is correlated with the uncertainty in future F_G, and these correlated uncertainties largely compensate. In evaluating ρ and the TCR (section 2.1), we decided to omit from consideration the possible induced cloud forcing of CO_2 discussed by *Gregory and Webb* [2008] and *Andrews and Forster* [2008]. Since CO_2 is the dominant contribution to F_G, and provided this effect multiplies F_G by a constant ratio, it likewise will largely cancel out in the projections. Because $|F$ projected to increase and $|F_A|$ to decline, their ratio changes with time. If the ratio were constant, the forcing uncertainty would cancel out entirely in the projections of ΔT [*Allen et al.*, 2000].

[54] The 5–95% range for ΔT from 1990 to 2095 is 2.0–2.8 K, which lies within and is narrower than the 5–95% range of projections from a set of 19 CMIP3 AOGCMs, from which we obtain 1.9–3.4 K (treating the models as normally distributed) for the difference in mean ΔT from 1980–1999 to 2090–2099. Enlarging the uncertainty on ρ to take account of low, medium and high estimates for multidecadal unforced variability, following section 4.3, our projected range widens to 2.0–2.9 K, 1.7–3.1 K and 1.5–3.2 K respectively. These ranges are narrower than the likely range of 1.7–4.4 K from the assessment of *Meehl et al.* [2007] whose higher upper bound in particular reflects uncertainty in carbon cycle feedbacks that cannot be constrained from the past (section 7 and *Knutti et al.* [2008]).

6.3. Time-Dependence of Climate Resistance

[55] As we saw in section 2.1, $F \propto \Delta T$ is a good approximation in the 70 years of the 1% CO_2 experiments up to 2 × CO_2. However, deviations become apparent as the forcing continues to rise. After a further 70 years, the scenario reaches 4 × CO_2. The increase in F, and hence in ΔT, should be the same as in the first 70 years, i.e., the TCR. In fact, the warming during the second 70 years is greater in all the AOGCMs considered (Table 1). Examining N and $F - N$ shows that both κ and α tend to decrease (climate sensitivity rises, ocean heat uptake efficiency declines). (We calculate ΔT from 20-year means. For the first 70 years it is the mean for years 61–80. For the second 70 we use the difference between years 121–140 and 51–70; we cannot Centre a 20-year mean on year 140, since the 1% increase ends at year 140 in these experiments.) If the real world behaves qualitatively like this, projections made by scaling the TCR will tend to be underestimates; this is a possible explanation for our projections for A1B being lower than the AOGCM results. The underestimate would become more severe for projections further into the future, as the forcing rises. We note that in HadCM3 under SRES A1FI, the scenario with the strongest forcing, there is a tendency for ΔT to lie above the linear relationship in the 2090s (Figure 7).

7. Comparison With Optimal Fingerprinting

[56] In effect, this method of estimating ΔT for the future from ρ for the past is similar to scaling up the observed past ΔT by the ratio of future forcing to past forcing, i.e., $\Delta T_f = F_f/F_p\Delta T_p$ (f and p for "future" and "past"), which holds for constant ρ. A related idea has been employed by *Stott and Kettleborough* [2002] and *Stott et al.* [2006] in their observationally constrained projections, in which optimal fingerprinting methods (described by, e.g., *IDAG* [2005]) are used to estimate a factor by which an AOGCM simulation of the past should be scaled to agree with observations, to correct for errors in the modeled forcing and response. The same factor, with its uncertainty, is used to scale the AOGCM projection of the future, i.e., assuming that the fractional error in ΔT simulated by the AOGCM is time-independent.

[57] *Allen et al.* [2000] supported this assumption by considering the relationship between the temperature changes ΔT_1 and ΔT_2 at two times (with respect to an initial steady state $\Delta T = 0$) as simulated by a simple climate model for a range of α. Their "transfer function" (their Figure 2) is in effect a plot of ΔT_2 against ΔT_1 as α is varied. They find it to be a straight line. A straight line with slope F_2/F_1 is expected if $\Delta T \propto F$. Their result hence indicates that $F \propto \Delta T$ is a good approximation for their simple climate model. Its use to support optimal fingerprinting assumes that AOGCMs behave in the same way.

[58] *Kettleborough et al.* [2007] further investigated the applicability of this linear approximation using the simple climate model, and concluded that the nonlinearity of the transfer function has only a minor effect on the projections made by scaling AOGCM results for SRES scenarios. However, their results show that the scaling works better for some scenarios than others. The use of scaling factors from optimal fingerprinting must have some similar limitations to the assumption of constant climate resistance.

[59] Optimal fingerprinting is a more powerful technique than our regression of F against ΔT because it makes use of the spatiotemporal patterns of temperature change, not just the global mean. Furthermore, it derives separate scaling factors for individual forcing agents, such as greenhouse gases and anthropogenic aerosol, and therefore does not assume that the climate is equally responsive to all of them. On the other hand, the regression has the advantage of not depending on model simulations of climate change. It avoids the systematic uncertainty inherent in modeling by instead making the simple assumption that $\Delta T \propto F$. Apart from the dependence on scenario already discussed, this relationship will be inaccurate if climate feedbacks emerge in the future that have not been observed in the past, for instance from nonlinear increases in carbon release from the biosphere or rapid weakening of the Atlantic meridional overturning circulation. However, this limitation applies equally to scaling based on optimal fingerprinting or to any other method of constraining projections using observations [*Allen et al.*, 2000; *Kettleborough et al.*, 2007].

8. Conclusions

[60] Observations and AOGCM simulations of twentieth-century climate change, and AOGCM experiments with steadily increasing radiative forcing F, indicate a linear relationship $F = \rho\Delta T$, where ΔT is the global mean surface air temperature change and ρ a constant "climate resistance". The latter is the sum of the climate feedback parameter α and the ocean heat uptake efficiency κ. In the CMIP3 AOGCMs, these two parameters have substantial and uncorrelated uncertainty, with α being about twice as large as κ on average. The climate resistance is related to the transient climate response according to $\rho = F_{2\times}/\mathrm{TCR}$, where $F_{2\times}$ is the radiative forcing due to doubled CO_2 concentration. This relationship is the analogue for time-dependent climate change of the relationship $\alpha = F_{2\times}/\Delta T_{2\times}$ between the climate feedback parameter and the equilibrium climate sensitivity $\Delta T_{2\times}$. The observational constraint on the climate resistance is much stronger than on the climate feedback parameter.

[61] In the real and simulated past record, deviations from the linear relationship $F \propto \Delta T$ occur in years strongly affected by volcanic forcing, to which ΔT responds comparatively weakly; further analysis would be useful of the different character of response to forcing which is episodic rather than multidecadal. Disregarding any trend caused by natural forcing, we estimate from the data of 1970–2006 by ordinary linear least squares regression that the real-world $\rho = 1.7$–2.6 W m^{-2} K^{-1} and the TCR is 1.5–2.1 K (5–95% uncertainty ranges). This range does not allow for the possible contribution to the observed ΔT of longer-period unforced variability, which can only be estimated using AOGCMs. When we incorporate a midrange estimate of this variability, obtained from the HadCM3 AOGCM, the TCR range is enlarged to 1.3–2.3 K. making it comparable to the CMIP3 AOGCM range of 1.2–2.4 K. The similarity of these ranges is notable because they are obtained from completely independent methods. Our range is not based on climate-change simulations, but uses only the observed ΔT and estimated past F.

[62] The systematic uncertainties in natural forcing and anthropogenic aerosol forcing may not be fully reflected in our stated range. A partial but possibly biased attempt to account for natural forcings gives a value of ρ about 20%, larger i.e., TCR about 20% smaller. Our range is similar to 1.5–2.8 K derived by *Stott et al.* [2006] by optimal fingerprinting (converted from their units of K century^{-1}), and to 1.1–2.3 K obtained by *Knutti and Tomassini* [2008] by applying constraints from observed ΔT and ocean heat uptake to a very large ensemble of simulations of the past and future made by varying parameters in a climate model of intermediate complexity. These methods use more information (the entire twentieth century, and geographical patterns of variables other than surface air temperature), so it may appear surprising that their results have no less uncertainty. One possible reason is the comparative insensitivity of our result to the large uncertainty in anthropogenic aerosol forcing, which was relatively constant during the period concerned, and therefore did not affect the trend in ΔT. Moreover, the relationship $F = \rho\Delta T$ suggests that the recent few decades, during which change has been largest, are most influential in the observational constraint on ρ and TCR.

[63] The linear relationship could not be expected to hold under all scenarios; in general, it should be a reasonable assumption for scenarios of fairly steadily increasing forcing, in which case $\kappa\Delta T$ is an acceptable approximation for ocean heat uptake. The value of ρ has some dependence on the scenario, so our empirical ρ is applicable only to scenarios with a rate of future forcing increase within a restricted range, similar to that of the recent past from which it was evaluated. Using $\Delta T = F/\rho$, we obtain projections for the warming during the twenty-first century under the SRES A1B scenario that have a similar range to those obtained from AOGCMs. The projections will be inaccurate if nonlinear or different climate feedbacks, not seen in the past, become important in the future [cf. *Knutti and Tomassini*, 2008]. The same applies to projections constrained by observations using optimal fingerprinting, which implicitly depend on $F \propto \Delta T$. The advantage of using this relationship explicitly is its simplicity, which permits some insight into the sources of uncertainty in projections.

[64] **Acknowledgments.** We thank Jim Haywood for the aerosol forcing PDF, Sarah Raper for the IPCC TAR time series, Reto Knutti, Peter Stott, Gabi Hegerl, and Gareth Jones for useful discussions and comments, and the referees for their reviews, which all helped to improve the paper. Jonathan Gregory was supported at the University of Reading by the National Centre for Atmospheric Science and at the Met Office by the Integrated Climate Programme, GA01101 (Defra) and CBC/2B/0417 Annex C5 (MoD). We thank the modeling groups, the Program for Climate Model Diagnosis and Intercomparison (PCMDI), and the WCRP's Working Group on Coupled Modeling for their roles in making available the WCRP CMIP3 multimodel data set. Support for this data set is provided by the Office of Science, U.S. Department of Energy.

References

Allen, M. R., P. A. Stott, J. F. B. Mitchell, R. Schnur, and T. L. Delworth (2000), Quantifying the uncertainty in forecasts of anthropogenic climate change, *Nature*, *407*, 617–620.

Andrews, T., and P. M. Forster (2008), CO_2 forcing induces semi-direct effects with consequences for climate feedback interpretations, *Geophys. Res. Lett.*, *35*, L04802, doi:10.1029/2007GL032273.

Bindoff, N. L., et al. (2007), Observations: Oceanic climate change and sea level, in *Climate Change 2007: The Physical Science Basis. Contribution of Working Group I to the Fourth Assessment Report of the Intergovernmental Panel on Climate Change*, edited by S. Solomon et al., Cambridge Univ. Press, Cambridge, United Kingdom and New York, NY, USA.

Boucher, O., and J. Haywood (2001), On summing the components of radiative forcing of climate change, *Clim. Dyn.*, *18*, 297–302.

Brohan, P., J. Kennedy, I. Harris, S. F. B. Tett, and P. D. Jones (2006), Uncertainty estimates in regional and global observed temperature changes: A new dataset from 1850, *J. Geophys. Res.*, *111*, D12106, doi:10.1029/2005JD006548.

Chylek, P., U. Lohmann, M. Dubey, M. Mishchenko, R. Kahn, and A. Ohmura (2007), Limits on climate sensitivity derived from recent satellite and surface observations, *J. Geophys. Res.*, *112*, D24S04, doi:10.1029/2007JD008740.

Collins, W. D. (2006), Radiative forcing by well-mixed greenhouse gases: Estimates from climate models in the Intergovernmental Panel on Climate Change (IPCC) Fourth Assessment Report (AR4), *J. Geophys. Res.*, *111*, D14317, doi:10.1029/2005JD006713.

Cubasch, U., G. A. Meehl, G. J. Boer, R. J. Stouffer, M. Dix, A. Noda, C. A. Senior, S. C. B. Raper, and K. S. Yap (2001), Projections of future climate change, in *Climate Change 2001: The Scientific Basis. Contribution of Working Group I to the Third Assessment Report of the Intergovernmental Panel on Climate Change*, edited by J. T. Houghton et al., pp. 525–582, Cambridge Univ. Press, Cambridge, United Kingdom and New York, NY, USA.

Dufresne, J.-L., and S. Bony (2008), An assessment of the primary sources of spread of global warming estimates from coupled atmosphere-ocean models, *J. Clim.*, *21*, 5134–5144, doi:10.1175/2008JCLI2239.1.

Forest, C. E., P. H. Stone, and A. P. Sokolov (2006), Estimated PDFs of climate system properties including natural and anthropogenic forcings, *Geophys. Res. Lett.*, *33*, L01705, doi:10.1029/2005GL023977.

Forster, P. M. de F., and M. Collins (2004), Quantifying the water vapour feedback associated with post-Pinatubo global cooling, *Clim. Dyn.*, *23*, 207–214.

Forster, P. M. de F., and J. M. Gregory (2006), The climate sensitivity and its components diagnosed from Earth radiation budget data, *J. Clim.*, *19*, 39–52.

Forster, P. M. de F., and K. E. Taylor (2006), Climate forcings and climate sensitivities diagnosed from coupled climate model integrations, *J. Clim.*, *19*, 6181–6194.

Forster, P., et al. (2007), Changes in atmospheric constituents and in radiative forcing, in *Climate Change 2007: The Physical Science Basis. Contribution of Working Group 1 to the Fourth Assessment Report of the Intergovernmental Panel on Climate Change*, edited by S. Solomon et al., pp. 129–234, Cambridge Univ. Press, Cambridge, United Kingdom.

Frame, D. J., B. B. B. Booth, J. A. Kettleborough, D. A. Stainforth, J. M. Gregory, M. Collins, and M. R. Allen (2005), Constraining climate forecasts: The role of prior assumptions, *Geophys. Res. Lett.*, *32*, L09702, doi:10.1029/2004GL022241.

Gordon, C., C. Cooper, C. A. Senior, H. Banks, J. M. Gregory, T. C. Johns, J. F. B. Mitchell, and R. A. Wood (2000), The simulation of SST, sea ice extents and ocean heat transports in a version of the Hadley Centre coupled model without flux adjustments, *Clim. Dyn.*, *16*, 147–168.

Gregory, J. M., and J. F. B. Mitchell (1997), The climate response to CO_2 of the Hadley Centre coupled AOGCM with and without flux adjustment, *Geophys. Res. Lett.*, *24*, 1943–1946.

Gregory, J. M., and M. J. Webb (2008), Tropospheric adjustment induces a cloud component in CO_2 forcing, *J. Clim.*, *21*, 58–71.

Gregory, J. M., R. J. Stouffer, S. C. B. Raper, P. A. Stott, and N. A. Rayner (2002), An observationally based estimate of the climate sensitivity, *J. Clim.*, *15*, 3117–3121.

Gregory, J. M., W. J. Ingram, M. A. Palmer, G. S. Jones, P. A. Stott, R. B. Thorpe, J. A. Lowe, T. C. Johns, and K. D. Williams (2004), A new method for diagnosing radiative forcing and climate sensitivity, *Geophys. Res. Lett.*, *31*, L03205, doi:10.1029/2003GL018747.

Gregory, J. M., J. A. Lowe, and S. F. B. Tett (2006), Simulated global mean sea-level changes over the last half-millennium, *J. Clim.*, *19*, 4576–4591.

Hansen, J., et al. (2005), Efficacy of climate forcings, *J. Geophys. Res.*, *110*, D18104, doi:10.1029/2005JD005776.

Hasselmann, K., R. Sausen, E. Maier-Reimer, and R. Voss (1993), On the cold start problem in transient simulations with coupled atmosphere-ocean models, *Clim. Dyn.*, *9*, 53–61.

Haywood, J., and M. Schulz (2007), Causes of the reduction in uncertainty in the anthropogenic radiative forcing of climate between IPCC (2001) and IPCC (2007), *Geophys. Res. Lett.*, *34*, L20701, doi:10.1029/2007GL030749.

Hegerl, G. C., F. W. Zwiers, P. Braconnot, N. P. Gillett, Y. Luo, J. A. M. Orsini, N. Nicholls, J. E. Penner, and P. A. Stott (2007), Understanding and attributing climate change, in *Climate Change 2007: The Physical Science Basis. Contribution of Working Group I to the Fourth Assessment Report of the Intergovernmental Panel on Climate Change*, edited by S. Solomon et al., Cambridge Univ. Press, Cambridge, United Kingdom.

Huntingford, C., and P. M. Cox (2000), An analogue model to derive additional climate change scenarios from existing GCM simulations, *Clim. Dyn.*, *16*, 575–586.

International Ad Hoc Detection and Attribution Group (IDAG) (2005), Detecting and attributing external influences on the climate system: A review of recent advances, *J. Clim.*, *18*, 1291–1341, doi:10.1175/JCLI3329.1.

Johns, T. C., et al. (2003), Anthropogenic climate change for 1860 to 2100 simulated with the HadCM3 model under updated emissions scenarios, *Clim. Dyn.*, *20*, 583–612, doi:10.1007/s00382-002-0296-y.

Keen, A. B., and J. M. Murphy (1997), Influence of natural variability and the cold start problem on the simulated transient response to increasing CO_2, *Clim. Dyn.*, *13*, 847–864.

Kettleborough, J. A., B. B. B. Booth, P. A. Stott, and M. R. Allen (2007), Estimates of uncertainty in predictions of global mean surface temperature, *J. Clim.*, *20*, 843–855.

Knutti, R., and L. Tomassini (2008), Constraints on the transient climate response from observed global temperature and ocean heat uptake, *Geophys. Res. Lett.*, *35*, L09701, doi:10.1029/2007GL032904.

Knutti, R., F. Joos, S. A. Muller, G. K. Plattner, and T. F. Stocker (2005), Probabilistic climate change projections for CO_2 stabilization profiles, *Geophys. Res. Lett.*, *32*, L20707, doi:10.1029/2005GL023294.

Knutti, R., et al. (2008), A review of uncertainties in global temperature projections over the twenty-first century, *J. Clim.*, *21*, 2651–2663, doi:10.1175/2007JCLI2119.1.

Levitus, S., J. I. Antonov, J. Wang, T. L. Delworth, K. W. Dixon, and A. J. Broccoli (2001), Anthropogenic warming of the Earth's climate system, *Science*, *292*, 267–270.

Meehl, G. A., et al. (2007), Global climate projections, in *Climate Change 2007: The Physical Science Basis. Contribution of Working Group I to the Fourth Assessment Report of the Intergovernmental Panel on Climate Change*, edited by S. Solomon et al., Cambridge Univ. Press, Cambridge, United Kingdom and New York, NY, USA.

Mitchell, J. F. B., T. C. Johns, M. Eagles, W. J. Ingram, and R. A. Davis (1999), Towards the construction of climate change scenarios, *Clim. Change*, *41*, 547–581.

Myhre, G., E. J. Highwood, K. P. Shine, and F. Stordal (1998), New estimates of radiative forcing due to well mixed greenhouse gases, *Geophys. Res. Lett.*, *25*, 2715–2718.

Myhre, G., A. Myhre, and F. Stordal (2001), Historical evolution of radiative forcing of climate, *Atmos. Environ.*, *35*, 2361–2373.

Nakićenović, N., et al. (2000), *Special Report on Emissions Scenarios*, edited by S. Solomon et al., 599 pp., Cambridge Univ. Press, Cambridge, United Kingdom.

Plattner, G.-K., et al. (2008), Long-term climate commitments projected with climate-carbon cycle models, *J. Clim.*, 2721–2751.

Press, W. H., S. A. Teukolsky, W. T. Vetterling, and B. P. Flannery (1992), *Numerical Recipes in Fortran: The Art of Scientific Computing*, 2nd ed., Cambridge Univ. Press, Cambridge, U.K.

Randall, D. A., et al. (2007), Climate models and their evaluation, in *Climate Change 2007: The Physical Science Basis. Contribution of Working Group I to the Fourth Assessment Report of the Intergovernmental Panel on Climate Change*, chap. 8, edited by S. Solomon et al., pp. 589–662, Cambridge Univ. Press, Cambridge, United Kingdom.

Raper, S. C. B., J. M. Gregory, and R. J. Stouffer (2002), The role of climate sensitivity and ocean heat uptake on AOGCM transient temperature response, *J. Clim.*, *15*, 124–130.

Shine, K. P., J. Cook, E. J. Highwood, and M. M. Joshi (2003), An alternative to radiative forcing for estimating the relative importance of climate change mechanisms, *Geophys. Res. Lett.*, *30*(20), 2047, doi:10.1029/2003GL018141.

Spencer, R. W., and W. D. Braswell (2008), Potential biases in feedback diagnosis from observational data: A simple model demonstration, *J. Clim.*, *21*, 5624–5628, doi:10.1175/2008JCLI2253.1.

Stott, P. A., and J. A. Kettleborough (2002), Origins and estimates of uncertainty in predictions of twenty first century temperature rise, *Nature*, *416*, 723–726.

Stott, P. A., S. F. B. Tett, G. S. Jones, M. R. Allen, J. F. B. Mitchell, and G. J. Jenkins (2000), External control of twentieth century temperature by natural and anthropogenic causes, *Science*, *290*, 2133–2137.

Stott, P. A., J. F. B. Mitchell, M. R. Allen, T. L. Delworth, J. M. Gregory, G. A. Meehl, and B. D. Santer (2006), Observational constraints on past attributable warming and predictions of future global warming, *J. Clim.*, *19*, 3055–3069.

Stouffer, R. J., and S. Manabe (1999), Response of a coupled ocean-atmosphere model to increasing atmospheric carbon dioxide: Sensitivity to the rate of increase, *J. Clim.*, *12*, 2224–2237.

Wang, Y. M., J. L. Lean, and N. R. Sheeley (2005), Modeling the sun's magnetic field and irradiance since 1713, *Astrophys. J.*, *625*, 522–538.

Watterson, I. G. (2000), Interpretation of simulated global warming using a simple model, *J. Clim.*, *13*, 202–215.

Williams, K. D., W. J. Ingram, and J. M. Gregory (2008), Time variation of effective climate sensitivity in GCMs, *J. Clim.*, *21*, 5076–5090, doi:10.1175/2008JCLI2371.1.

P. M. Forster, School of Earth and Environment, University of Leeds, LS2 9JT Leeds, UK. (p.m.forster@leeds.ac.uk)

J. M. Gregory, Department of Meteorology, Walker Institute for Climate System Research, University of Reading, Meteorology Building, P.O. Box 243, RG1 5RY Reading, UK. (j.m.gregory@reading.ac.uk)